Nature of the phases in the frustrated *XY* model on the honeycomb lattice

Juan Carrasquilla,[1,2] Andrea Di Ciolo,[3,2] Federico Becca,[4,5] Victor Galitski,[3] and Marcos Rigol[1]

[1]*Department of Physics, The Pennsylvania State University, University Park, Pennsylvania 16802, USA*
[2]*Department of Physics, Georgetown University, Washington, DC 20057, USA*
[3]*Joint Quantum Institute and Department of Physics, University of Maryland, College Park, Maryland 20742, USA*
[4]*Democritos Simulation Center CNR-IOM Istituto Officina dei Materiali, Trieste, Italy*
[5]*International School for Advanced Studies (SISSA), Via Beirut 2, I-34151, Trieste, Italy*

We study the phase diagram of the frustrated *XY* model on the honeycomb lattice by using accurate correlated wave functions and variational Monte Carlo simulations. Our results suggest that a spin-liquid state is energetically favorable in the region of intermediate frustration, intervening between two magnetically ordered phases. The latter ones are represented by classically ordered states supplemented with a long-range Jastrow factor, which includes relevant correlations and dramatically improves the description provided by the purely classical solution of the model. The construction of the spin-liquid state is based on a decomposition of the underlying bosonic particles in terms of spin-1/2 fermions (partons), with a Gutzwiller projection enforcing no single occupancy, as well as a long-range Jastrow factor.

A quantum spin liquid is an exotic state in which strong quantum fluctuations (usually generated by frustration) preclude ordering or freezing, even at zero temperature.[1] Despite intensive theoretical and experimental research, finding quantum spin liquids in materials and in realistic spin models continues to be a challenge. A remarkable example where the existence of such a state has been inferred is the spin-1/2 kagome-lattice Heisenberg antiferromagnet, which has been extensively studied both theoretically and experimentally,[1–3] even though the precise nature of the ground state of the system is still under debate.[3–6] Furthermore, recent studies[7–10] have also analyzed exactly solvable Kagome lattice spin-liquid models.

Another model that has recently received considerable attention for its potential to realize spin-liquid states is the spin-1/2 Heisenberg model on the honeycomb lattice, with nearest-neighbor (NN) J_1 and next-to-nearest neighbor (NNN) J_2 exchange interactions.[11–20] This is in part motivated by its close relation to the Hubbard model, for which the possibility of having a spin-liquid ground state has been under close scrutiny.[21–23]

A closely related spin model with a rich phase diagram and the promise to support a gapless spin liquid phase is the $J_1 - J_2$ spin-1/2 *XY* model on the honeycomb lattice,[24,25] which is the main subject of this Rapid Communication. Its Hamiltonian can be written as

$$\mathcal{H} = J_1 \sum_{\langle ij \rangle} \left(S_i^x S_j^x + S_i^y S_j^y \right) + J_2 \sum_{\langle\langle ij \rangle\rangle} \left(S_i^x S_j^x + S_i^y S_j^y \right), \quad (1)$$

where S_i^α is the αth component of the spin-1/2 operator at site i. This model can be thought of as a Haldane-Bose-Hubbard model,[24,26–28] i.e., the Haldane model[29] on the honeycomb lattice with NN hopping J_1 and complex NNN hopping $|J_2|e^{i\phi}$, where spinless fermions are replaced by hard-core bosons and $\phi = 0$. Hard-core boson creation and annihilation operators can then be mapped onto spin operators ($b_i^\dagger \rightarrow S_i^+$, $b_i \rightarrow S_i^-$) leading to Eq. (1). The total number of bosons (N) is related to the total magnetization in the spin language, since
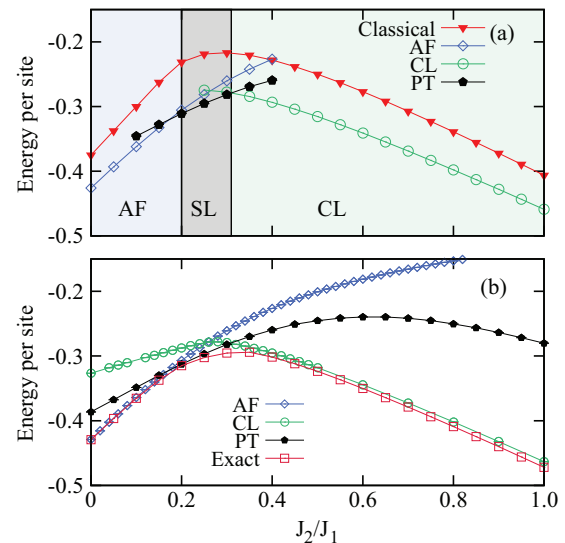

FIG. 1. (Color online) (a) Extrapolated best energies in the thermodynamic limit, as well as the final phase diagram (colored regions labeled AF, SL, and CL) based on the properties of the states considered. The energy of the purely classical solution of the model is shown for comparison. (b) Energies of antiferromagnetic and spin-liquid states compared to the exact results on the $4 \times 4 \times 2$ cluster.

$n_i = S_i^z + 1/2$. Here, we focus on the half-filled case, where N equals one-half the number of sites (V).

This model was studied in Ref. 24 by means of exact diagonalization on small clusters. There, evidence was found supporting the existence of a spin liquid surrounded by two magnetically ordered states, namely, an antiferromagnetic (collinear) state at lower (higher) J_2/J_1. The spin-liquid phase was suggested to be gapless and characterized by a distinctive parameter dependent feature in the momentum distribution $n(\mathbf{k})$, similar to a Bose surface, thus suggesting the presence of an exotic Bose metal.[24,28,30–35]

Here, we study the phase diagram of the $J_1 - J_2$ spin-1/2 XY model on the honeycomb lattice using variational Monte Carlo (VMC). By utilizing an accurate, yet simple and intuitive representation of magnetically ordered states, we find that the system remains in the antiferromagnetic (AF) phase for $0 \leqslant J_2/J_1 \leqslant 0.2$, while a collinear (CL) state stabilizes for $0.3 \lessapprox J_2/J_1 \lessapprox 1.1$. The accuracy of our representation, tested against exact diagonalization results on small clusters, is unprecedented. In the intermediate region $0.2 \lessapprox J_2/J_1 \lessapprox 0.3$, we find that the ordered phases have a higher energy than a fractionalized partonic state, which is consistent with a gapped spin liquid. The variational energy of such a state is gauged against a wide range of carefully optimized magnetically ordered spin states, as well as states that allow the breaking of spatial symmetries. Extrapolations of energy to the thermodynamic limit of the best trial states, as well as the phase diagram of the model, are presented in Fig. 1. The energy of the purely classical solution of the model is shown to make apparent the importance of introducing quantum fluctuations in our trial states.

As trial wave functions for the magnetically ordered states, we use classical spin-waves on the XY plane supplemented with long-range Jastrow factors:

$$|\Psi_{\mathbf{Q}}\rangle = \mathcal{J}_z \prod_i (|\downarrow\rangle_i + e^{\iota \mathbf{Q} \cdot \mathbf{R}_i + \iota \eta_{\mathbf{R}_i}} |\uparrow\rangle_i), \qquad (2)$$

where i runs over the positions of the spins, $\mathbf{Q}$ is the wave vector of the classical spin wave, and $\eta_{\mathbf{R}_i}$ is the phase shift between the two spins within the unit cell. Without loss of generality, we assume $\eta_{\mathbf{R}_i} = 0$ if $\mathbf{R}_i$ belongs to the sublattice $\mathcal{A}$ and an arbitrarily chosen $\eta_{\mathbf{R}_i} = \eta$ if it belongs to the sublattice $\mathcal{B}$. The long-range Jastrow factor $\mathcal{J}_z = \exp(\frac{1}{2} \sum_{i,j} v_{ij} S_i^z S_j^z)$, with v_{ij} to be optimized, is also considered to include relevant (i.e., out-of-plane) quantum correlations. In the bosonic language, the magnetically ordered states are nothing but condensates where particles macroscopically populate finite-$\mathbf{Q}$ momentum states.

The trial wave function for the intermediate spin-liquid state is written as

$$|\Psi_{\mathrm{SL}}\rangle = \mathcal{J}_z P_G |\Psi_{c_\uparrow, c_\downarrow}\rangle, \qquad (3)$$

where $|\Psi_{c_\uparrow, c_\downarrow}\rangle$ is the ground state of a free-fermion Hamiltonian

$$\mathcal{H}_{c_\uparrow, c_\downarrow} = \sum_{\langle i,j \rangle} \Psi_i^\dagger T_{\mathrm{NN}}^{ij} \Psi_j + \sum_{\langle\langle i,j \rangle\rangle} \Psi_i^\dagger T_{\mathrm{NNN}}^{ij} \Psi_j + \sum_i \Psi_i^\dagger M^i \Psi_i,$$
$$(4)$$

in which $\Psi_i^\dagger = (c_{\uparrow,i}^\dagger, c_{\downarrow,i}^\dagger)$ acts at site i and is composed by two fermions (partons) $c_{\uparrow,i}^\dagger$ and $c_{\downarrow,i}^\dagger$. The latter ones are related to the underlying physical hard-core bosons (or spin-1/2 operators) via $b_i^\dagger = c_{\uparrow,i}^\dagger c_{\downarrow,i}^\dagger$. The matrices

$$T_n^{ij} = \begin{bmatrix} t_{ij}^\uparrow & t_{ij}^s + t_{ij}^a \\ t_{ij}^{s*} - t_{ij}^{a*} & t_{ij}^\downarrow \end{bmatrix}, \quad M^i = \begin{bmatrix} m_i^{\uparrow\uparrow} & m_i^{\uparrow\downarrow} \\ m_i^{\uparrow\downarrow*} & m_i^{\downarrow\downarrow} \end{bmatrix}$$
$$(5)$$

contain hopping parameters and on-site couplings ($n = \mathrm{NN}$ and NNN). In order to have a state that lives in the correct

Hilbert space (with one spin per site), a Gutzwiller projector P_G must be introduced, imposing no single occupancy for fermions. Furthermore, a long-range Jastrow factor $\mathcal{J}_z$ is also considered. The Jastrow factors, as well as all parameters in Eq. (4), are carefully optimized using VMC methods as described in Refs. 36 and 37. After imposing particle-hole (PH) symmetry in the variational ansatz (4), the most energetically favorable mean-field state is found to have real NN hopping $t_{ij}^\uparrow = -t_{ij}^\downarrow = t = 1$, as well as nonvanishing complex on-site $m_i^{\uparrow\downarrow}$ and real NNN "spin-orbit" hopping $t_{ij}^s = t_{ij}^{s*}$, while $t_{i,j}^a = m_i^{\downarrow\downarrow} = m_i^{\uparrow\uparrow} = 0$. Note that, at half filling, PH symmetry $b_j^\dagger \to b_j$ in the bosonic language (i.e., $c_{\uparrow,j}^\dagger \to -\iota c_{\downarrow,j}$ and $c_{\downarrow,j}^\dagger \to \iota c_{\uparrow,j}$) implies that both T_n^{ij} and M^i must be written in terms of Pauli matrices, which reduces the total number of independent parameters.

In Fig. 1, we present results for the energy vs J_2/J_1 on a $4 \times 4 \times 2$ cluster and compare them with those obtained from exact diagonalization. For $J_2/J_1 \lessapprox 0.2$ ($J_2/J_1 \gtrapprox 0.35$), the best variational states are given by Eq. (2) with $\mathbf{Q} = \Gamma$ ($\mathbf{Q} = M$) and a phase shift $\eta = \pi$ ($\eta = 0$). They correspond to antiferromagnetic states with collinear order. These two ordered states surround an intermediate region where a state constructed from Eq. (4) possesses the best variational energy. The discrepancy in the energy of our trial states with respect to results from exact diagonalization is always less than 3%, except for $J_2/J_1 = 0.3$ for which it is ~4%.[38]

For larger cluster sizes, we have analyzed an extensive set of possible states. For the classically ordered states, we minimized the energy for a large number of spin waves generated by nonequivalent $\mathbf{Q}$ vectors and for a dense grid of values of η. For spin-wave states with generic pitch vectors $\mathbf{Q}$, it is important to allow for Jastrow factors that break rotational symmetry. Regarding the projected fermionic ansatz, we have considered translationally and rotationally invariant states and also allowed for breaking spatial symmetries. We have done that by considering enlarged unit cells that contain 4 and 18 sites, as well as states in which the couplings of the mean-field Hamiltonian form plaquettelike structures, and fermionic states supplemented with a $\mathcal{J}_z$ such that the breaking of rotational invariance is allowed. Within that set of fermionic trial wave functions, the state with lowest energy, as the system size is increased, is such that no spatial symmetries in both $\mathcal{J}_z$ and $\mathcal{H}_{c_\uparrow, c_\downarrow}$ are broken.[38]

Within the magnetic states described by the ansatz of Eq. (2), we find that quantum fluctuations (accounted for by $\mathcal{J}_z$) stabilize the antiferromagnetic (AF) phase for larger values of J_2/J_1 with respect to the classical solution. Indeed, the $\mathbf{Q} = \Gamma$ ($\eta = \pi$) state remains lower than other spin-wave states up to $J_2/J_1 \approx 0.25$ (to be compared to $J_2/J_1 = 1/6$ for the classical solution). Similar results were obtained for the $J_1 - J_2$ spin-1/2 Heisenberg model on the honeycomb lattice.[18] Furthermore, for $0.25 \lessapprox J_2/J_1 \lessapprox 1.1$, the best magnetic state has collinear (CL) order, with $\mathbf{Q} = M$ and $\eta = 0$. This outcome is in contrast with the classical limit, where states with incommensurate order are found. Most importantly, among all states of the form (2) in the clusters considered, no single quantum spin wave has lower energy in the intermediate J_2/J_1 region than that of the state based on Eq. (4).
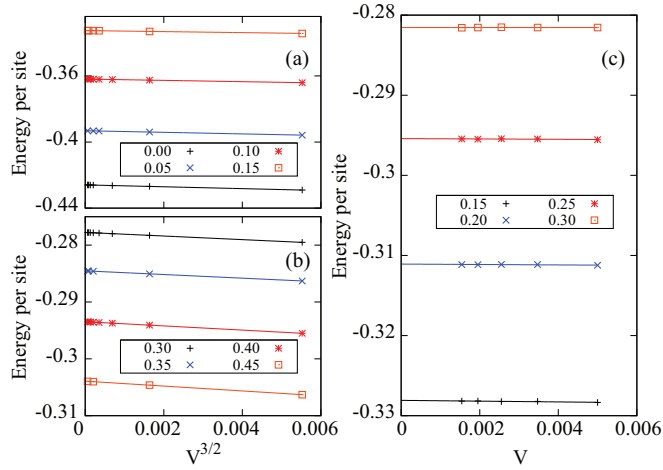
FIG. 2. (Color online) Finite-size scaling of the AF energies (a), the CL states (b), and projected fermionic states (c). In the legends, the numbers indicate values of J_2/J_1.

The trends discussed above are confirmed by simulations on clusters with sizes up to $18 \times 18 \times 2$, and in extrapolations of the energies to the thermodynamic limit, as presented in Fig. 1. We expect finite size corrections to the energy e_0 in the AF phase to be of the form $e_0(V) = e_0(\infty) - c_0/V^{3/2}$,[39] [see Fig. 2(a)] where the slope c_0 is proportional to the velocity of the AF spin wave. The latter (not shown) decreases approximately linearly with increasing frustration (for small frustration), as in the AF phase of the frustrated Heisenberg model on the same geometry.[40] The aforementioned scaling relation describes the data in the CL phase as displayed in Fig. 2(b). Finally, for the projected fermionic state, we assume the simple form $e_0(V) = e_0(\infty) - d_0/V$ to extract $e_0(\infty)$ as reported in Fig. 2(c).

In what follows, we study the properties of the projected fermionic state that bears the lowest energy at intermediate frustration. After minimizing the energy on several clusters, the resulting ansatz $|\Psi_{c_\uparrow,c_\downarrow}\rangle$ was found to have a gap to single-particle fermionic excitations Δ as shown in Fig. 3(a) for a $18 \times 18 \times 2$ cluster. The corresponding unprojected band structure for $J_2/J_1 = 0.25$ (four bands) is shown in Fig. 3(b).
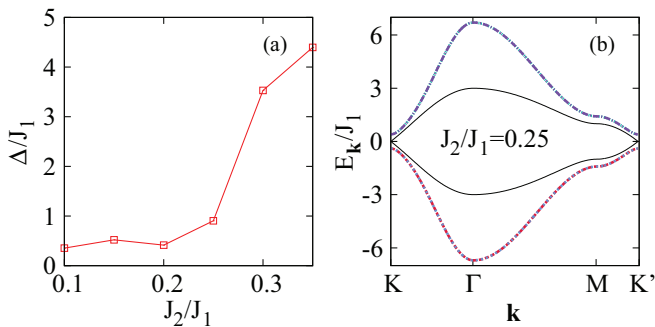

FIG. 3. (Color online) (a) Single-particle gap of the optimized fermionic Hamiltonian in Eq. (4) as a function of J_2/J_1 for the $18 \times 18 \times 2$ cluster. (b) The unprojected band structure for $J_2/J_1 = 0.25$. For comparison, black solid lines show the band structure for real NN hopping only.
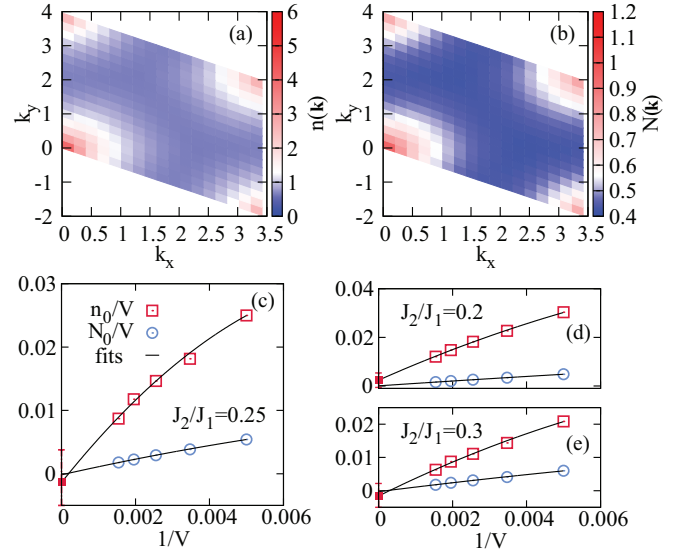

FIG. 4. (Color online) Momentum distribution $n(\mathbf{k})$ (a) and Static structure factor $N(\mathbf{k})$ (b) for $J_2/J_1 = 0.25$ on the $18 \times 18 \times 2$ cluster. Finite size scaling of the condensate fraction n_0/V and N_0/V for $J_2/J_1 = 0.25$ (c), $J_2/J_1 = 0.2$ (d), and $J_2/J_1 = 0.3$ (e). The solid lines correspond to fits of the data to a second-order polynomial. The corresponding extrapolation of the condensate fraction is shown with filled red squares.

Whether the system possesses magnetic order is assessed calculating the momentum distribution function $n^{\alpha,\beta}(\mathbf{k})$, where α and β denote the two sites inside the unit cell [i.e., $n^{\alpha,\beta}(\mathbf{k})$ is a 2×2 matrix]. In Fig. 4(a), we report the trace $n(\mathbf{k}) = \text{tr}[n^{\alpha,\beta}(\mathbf{k})]$ of this matrix for $J_2/J_1 = 0.25$. We find a clear peak at the Γ point, which might suggest that the resulting state is still antiferromagnetically ordered. However, upon a finite-size scaling analysis of the condensate fraction n_0/V, where n_0 is the largest eigenvalue of the one-body density matrix ($\langle b_i^\dagger b_j \rangle$ in the bosonic language or $\langle S_i^+ S_j^- \rangle$ in the spin language), we find that the state is not ordered in the thermodynamic limit. Figure 4(c) shows the evolution of n_0/V for $J_2/J_1 = 0.25$, as the system size is increased. The solid black line corresponds to a fit to a second-order polynomial, which makes apparent that n_0/V vanishes as $V \to \infty$ (within the error bar of the fit). Figures 4(d) and 4(e) also make apparent that the same happens in the boundaries of the region where the partonic state has the lowest energy.

We have also evaluated the structure factor $N^{\alpha,\beta}(\mathbf{k})$ (in which the constant $\mathbf{k} = 0$ term has been subtracted), to look for diagonal ordering in our projected fermionic ansatz. Results for the trace of $N(\mathbf{k}) = \text{tr}[N^{\alpha,\beta}(\mathbf{k})]$ for $J_2/J_1 = 0.25$ are displayed in Fig. 4(b). Also in this case, we find a clear peak at the Γ point. In order to understand whether this corresponds to diagonal order, we performed a finite-size scaling analysis of the ratio N_0/V, where N_0 is the largest eigenvalue of the diagonal two-body correlation function ($\langle n_i n_j \rangle - \langle n_i \rangle \langle n_j \rangle$ in the bosonic language, $\langle S_i^z S_j^z \rangle - \langle S_i^z \rangle \langle S_j^z \rangle$ in the spin language). Results for N_0/V, are shown in Figs. 4(c)–4(e) for $J_2/J_1 = 0.20, 0.25$ and $J_2/J_1 = 0.3$, respectively. They extrapolate to zero in the thermodynamic limit, which means that there is no charge order associated with the peak of $N(\mathbf{k})$. Hence we

conclude that the ground state for $0.20 \lesssim J_2/J_1 \lesssim 0.3$ is likely to be a spin liquid.

A comparison of the results of this study with those of Ref. 24, reveals a very good agreement between the phase diagrams reported. However, there are important differences. The resulting momentum distribution in Fig. 4(a) does not exhibit a Bose surface, but instead a clear peak at Γ. Since such trial states are known to be capable of reproducing Bose surfaces, one possibility is that the Bose surface seen in the exact calculations will fade away as the system size increases. However, since the absence of a Bose surface in our ansatz holds also for small system sizes, another possibility is that we have not found the trial state that is able to capture such a feature, and which may ultimately exhibit a lower energy than the one reported here.

At this stage, the nature of the phase that we refer to as a "spin liquid" remains largely a mystery. The original exact diagonalization study[24] found a state that was consistent with a gapless spin liquid. This scenario is still in the running, however, the cluster sizes available to such studies are too small to make an unambiguous conclusion. On the other hand, our results for state (4) are consistent with a gapped spin liquid, clearly in contrast to the projected spinon Fermi surface state suggested in Ref. 24. In spite of the difficulties, in this work, we have been able to safely rule out straightforward magnetically ordered phases and spirals as competing ground states in the interesting region where the fractionalized spin-liquid state was found to win.

We note that it might be possible to reconcile the differences observed by recalling the arguments in Ref. 41. There, it was suggested that, just like a Landau Fermi liquid can be viewed as a parent state subject to various instabilities (e.g.,

superconductivity, Stoner ferromagnetism, or density waves), the U(1) projected Fermi liquid may serve as a parent state to a variety of Mott insulating states and gapped spin liquids. Such scenarios have been discussed in the literature: a density wave instability[42] and a superconducting instability,[41] which may be consistent with the state we discuss here by virtue of its close relation with projected BCS states previously studied in Refs. 12,13 and 20. In both cases, the nature of the possible instabilities hinges on the Friedel-like oscillations (or Kohn anomaly), which is produced by the fermionized bosons in the parent state. The existence of such oscillations can potentially be probed in numerical simulations of models with defects and would shed light on the true nature of the underlying state.

In summary, we have performed a variational study of the frustrated XY model on the honeycomb lattice. We have been able to map out all ordered phases and describe them with variational states with an unprecedented precision on lattices that for practical purposes represent thermodynamic limit (to which we believe there is no analog in the existing literature). We have also found that in the region $0.2 \lesssim J_1/J_2 \lesssim 0.3$, the ordered phases lose in energy to an exotic fractionalized partonic wave-function that is consistent with a gapped spin liquid. However, more work is needed to conclusively determine the true physical nature of the ground state of the system in this region.

[1] L. Balents, Nature (London) **464**, 199 (2010).

[2] S. Yan, D. A. Huse, and S. R. White, Science **332**, 1173 (2011).

[3] T.-H. Han, J. S. Helton, S. Chu, D. G. Nocera, J. A. Rodriguez-Rivera, C. Broholm, and Y. S. Lee, Nature (London) **492**, 406 (2012).

[4] L. Messio, B. Bernu, and C. Lhuillier, Phys. Rev. Lett. **108**, 207204 (2012).

[5] S. Depenbrock, I. P. McCulloch, and U. Schollwöck, Phys. Rev. Lett. **109**, 067201 (2012).

[6] Y. Iqbal, F. Becca, S. Sorella, and D. Poilblanc, Phys. Rev. B **87**, 060405 (2013).

[7] A. Seidel, Phys. Rev. B **80**, 165131 (2009).

[8] J. Wildeboer and A. Seidel, Phys. Rev. B **83**, 184430 (2011).

[9] N. Schuch, D. Poilblanc, J. I. Cirac, and D. Pérez-García, Phys. Rev. B **86**, 115108 (2012).

[10] F. Yang and H. Yao, Phys. Rev. Lett. **109**, 147209 (2012).

[11] F. Wang, Phys. Rev. B **82**, 024419 (2010).

[12] Y.-M. Lu and Y. Ran, Phys. Rev. B **84**, 024420 (2011).

[13] B. K. Clark, D. A. Abanin, and S. L. Sondhi, Phys. Rev. Lett. **107**, 087204 (2011).

[14] H. Mosadeq, F. Shahbazi, and S. A. Jafari, J. Phys.: Condens. Matter **23**, 226006 (2011).

[15] A. F. Albuquerque, D. Schwandt, B. Hetényi, S. Capponi, M. Mambrini, and A. M. Läuchli, Phys. Rev. B **84**, 024406 (2011).

[16] R. F. Bishop, P. H. Y. Li, D. J. J. Farnell, and C. E. Campbell, J. Phys.: Condens. Matter **24**, 236002 (2012).

[17] F. Mezzacapo and M. Boninsegni, Phys. Rev. B **85**, 060402 (2012).

[18] R. Ganesh, J. van den Brink, and S. Nishimoto, Phys. Rev. Lett. **110**, 127203 (2013).

[19] Z. Zhu, D. A. Huse, and S. R. White, Phys. Rev. Lett. **110**, 127205 (2013).

[20] S.-S. Gong, D. N. Sheng, O. I. Motrunich, and M. P. Fisher, Phys. Rev. B **88**, 165138 (2013).

[21] Z. Y. Meng, T. C. Lang, S. Wessel, F. F. Assaad, and A. Muramatsu, Nature (London) **464**, 847 (2010).

[22] S. Sorella, Y. Otsuka, and S. Yunoki, Sci. Rep. **2**, 992 (2012).

[23] F. F. Assaad and I. F. Herbut, Phys. Rev. X **3**, 031010 (2013).

[24] C. N. Varney, K. Sun, V. Galitski, and M. Rigol, Phys. Rev. Lett. **107**, 077201 (2011).

[25] T. A. Sedrakyan, L. I. Glazman, and A. Kamenev, arXiv:1303.7272.

[26] C. N. Varney, K. Sun, M. Rigol, and V. Galitski, Phys. Rev. B **82**, 115125 (2010).

[27] Y.-F. Wang, Z.-C. Gu, C.-D. Gong, and D. N. Sheng, Phys. Rev. Lett. **107**, 146803 (2011).

[28] C. N. Varney, K. Sun, V. Galitski, and M. Rigol, New J. Phys. **14**, 115028 (2012).

[29] F. D. M. Haldane, Phys. Rev. Lett. **61**, 2015 (1988).

[30] A. Paramekanti, L. Balents, and M. P. A. Fisher, Phys. Rev. B **66**, 054526 (2002).

[31] P. Phillips and D. Dalidovich, Science **302**, 243 (2003).

[32] O. I. Motrunich and M. P. A. Fisher, Phys. Rev. B **75**, 235116 (2007).

[33] D. N. Sheng, O. I. Motrunich, and M. P. A. Fisher, Phys. Rev. B **79**, 205112 (2009).

[34] R. V. Mishmash, M. S. Block, R. K. Kaul, D. N. Sheng, O. I. Motrunich, and M. P. A. Fisher, Phys. Rev. B **84**, 245127 (2011).

[35] L. Dang, S. Inglis, and R. G. Melko, Phys. Rev. B **84**, 132409 (2011).

[36] S. Sorella, Phys. Rev. B **71**, 241103 (2005).

[37] S. Yunoki and S. Sorella, Phys. Rev. B **74**, 014408 (2006).

[38] See Supplemental Material at http://link.aps.org/supplemental/10.1103/PhysRevB.88.241109 for details on the accuracy of the different trial states used and results of the extrapolations to the thermodynamic limit.

[39] D. S. Fisher, Phys. Rev. B **39**, 11783 (1989).

[40] A. Mattsson, P. Fröjdh, and T. Einarsson, Phys. Rev. B **49**, 3997 (1994).

[41] V. Galitski and Y. B. Kim, Phys. Rev. Lett. **99**, 266403 (2007).

[42] B. L. Altshuler, L. B. Ioffe, A. I. Larkin, and A. J. Millis, Phys. Rev. B **52**, 4607 (1995).